

Studies

Sources of carbon supporting the fast growth of developing immature moso bamboo (*Phyllostachys edulis*) culms: inference from carbon isotopes and anatomy

Shitephen Wang^{*1, }, Daniel Epron^{1, }, Keito Kobayashi^{2, }, Satoru Takanashi^{2, } and Masako Dannoura^{1, }

¹Graduate School of Agriculture, Kyoto University, Kitashirakawa Oiwake-cho, Sakyo-ku, Kyoto 606-8502, Japan

²Kansai Research Centre, Forestry and Forest Products Research Institute, 68 Momoyamacho Nagaikyutaro, Fushimi-ku, Kyoto 612-0855, Japan

*Corresponding author's e-mail address: gn03138868@gmail.com

Plants, Ecosystems and Climate. Chief Editor: Mary Heskell

Associate Editor: Lee Kalcsits

Abstract

Phyllostachys edulis is a spectacularly fast-growing species that completes its height growth within 2 months after the shoot emerges without producing leaves (fast-growing period, FGP). This phase was considered heterotrophic, with the carbon necessary for the growth being transferred from the mature culms via the rhizomes, although previous studies observed key enzymes and anatomical features related to C₄-carbon fixation in developing culms. We tested whether C₄-photosynthesis or dark-CO₂ fixation through anaplerotic reactions significantly contributes to the FGP, resulting in differences in the natural abundance of $\delta^{13}\text{C}$ in bulk organic matter and organic compounds. Further, pulse-¹³CO₂-labelling was performed on developing culms, either from the surface or from the internal hollow, to ascertain whether significant CO₂ fixation occurs in developing culms. $\delta^{13}\text{C}$ of young shoots and developing culms were higher (–26.3 to –26.9 ‰) compared to all organs of mature bamboos (–28.4 to –30.1 ‰). Developing culms contained chlorophylls, most observed in the skin tissues. After pulse-¹³CO₂-labelling, the polar fraction extracted from the skin tissues was slightly enriched in ¹³C, and only a weak ¹³C enrichment was observed in inner tissues. Main carbon source sustaining the FGP was not assimilated by the developing culm, while a limited anaplerotic fixation of respired CO₂ cannot be excluded and is more likely than C₄-photosynthetic carbon fixation.

Keywords: Anaplerotic pathway; carbon isotope fractionation; $\delta^{13}\text{C}$ of carbon compounds; *Phyllostachys edulis*; pulse ¹³CO₂ labelling.

Introduction

Phyllostachys edulis is a large monocotyledon (Poaceae, subfamily Bambusoideae) commonly distributed in East Asia's temperate or subtropical mountains. The plant grows incredibly fast from young shoots emerging from the ground to mature bamboos (10–15 m high) within 60 days without producing leaves, the photosynthesising organs (Yen and Lee 2011). Young bamboo shoots are shoots covered by sheaths before 25 to 40 internodes about 7.5 cm in diameter simultaneously undergoing cell division (0.06 cells cell⁻¹ h⁻¹) and elongation (0.49 $\mu\text{m} \mu\text{m}^{-1} \text{h}^{-1}$). The cell division zone at the base of the internode is up to 2 cm, while the elongation zone, the upper part of the internodes, is up to 12 cm (Chen *et al.* 2022). The elongation is completed within 21–25 days, resulting in the rapid growth of the young developing culms, during which time a large amount of carbon is required (Chen *et al.* 2022), after which the senescence of the sheath occurs (Chen *et al.* 2021). The young culms accumulate three-fourths

of their final biomass during the initial 40 days of this fast-growing period (FGP) (Yen 2016). The carbohydrates required to support this fast growth are thought to be transported from mature bamboos (autotrophic stage) to young leafless bamboos (heterotrophic stage) via the leptomorph rhizome systems (Song *et al.* 2016; Wang *et al.* 2020; Zhai *et al.* 2022).

Phyllostachys edulis is a C₃ plant, based on plastome phylogenetic trees, like rice (subfamily Oryzoideae), its close relative (Bianconi *et al.* 2020). This is confirmed by the leaf isotope composition ($\delta^{13}\text{C}$) of *P. edulis* (Hanba *et al.* 2010). Roots or stems are, however, expected to be slightly enriched compared to leaves because of post-photosynthetic carbon fractionations (Badeck *et al.* 2005). Early wood in the tree rings of deciduous species is often enriched in ¹³C because the carbon used in early spring is remobilised from carbon reserve (e.g. enriched starch), while the production of late wood is more directly related to the current photosynthetic carbon assimilation (Damesin and Lelarge 2003; Helle and Schleser

Received: 19 December 2022; Editorial decision: 13 June 2023; Accepted: 29 June 2023

© The Author(s) 2023. Published by Oxford University Press on behalf of the Annals of Botany Company.

This is an Open Access article distributed under the terms of the Creative Commons Attribution License (<https://creativecommons.org/licenses/by/4.0/>), which permits unrestricted reuse, distribution, and reproduction in any medium, provided the original work is properly cited.

2004; Gessler *et al.* 2014). Although not yet studied, there are good reasons to think that developing culms of bamboos should also be enriched compared to the leaves of mature bamboos if the photosynthetic products of mature bamboos are used to build storage compounds that are then transferred to developing immature culms.

Different organs of the same species also possibly exhibit different patterns of photosynthesis even though a plant is commonly recognised as a single photosynthetic type (e.g. C₃ or C₄). For instance, leaves show the C₃ type and stems show C₄ carbon fixation in celery and tobacco (Hibberd and Quick 2002). Although previous studies have shown that C₄ enzymes are upregulated during the heterotrophic stage of developing culms, little is known about their contribution to the carbon gain of new-born bamboo culms during the FGP. Wang *et al.* (2012) observed that the parenchyma cells around the vascular bundles in the developing immature bamboo culms contained chloroplasts. Wang *et al.* (2021) then revealed that the genes of the important enzymes related to the C₄ carbon fixation, such as the phosphoenolpyruvate carboxylase (PEPC), the nicotinamide adenine dinucleotide phosphate-malate dehydrogenase (NADP-MDH) and the NADP-malic enzyme (NADP-ME), were upregulated during the FGP. Furthermore, they revealed the activity of these key enzymes in developing culms during the FGP, suggesting that the 2-mm-thick skin of culms operates the NADP-ME subtype of C₄ carbon fixation. Mature *P. edulis* is therefore a typical C₃ plant but C₄-like patterns may be present in developing culms. Carbon fixation may therefore not only occur in leaves, the autotrophic organ of mature bamboo, but also in developing culms during the FGP, which would result in a strong ¹³C enrichment of developing culm organic matter compared to the leaves of mature bamboos.

It is well known that heterotrophic plant organs, such as tree stems, can assimilate carbon and that the source of CO₂ is partially from respiration (Cernusak and Marshall 2000; Wittmann *et al.* 2005; Berveiller *et al.* 2007). Forty per cent of carbon loss by respiration can be reassimilated in the current-year stems of European beech for example (Damesin 2003). The ¹³C signature of the respired CO₂ is determined by the relative contributions of the decarboxylation related to the pyruvate dehydrogenase activity and those occurring during the Krebs cycle (isocitrate dehydrogenase and alpha-ketoglutarate dehydrogenase activities), leading to an apparent fractionation of up to 6 ‰ (Ghashghaie *et al.* 2003; Tcherkez *et al.* 2003). Carbon fixation in tree stems can occur in darkness (Höll 1974; Langenfeld-Heyser 1989), which suggests the recycling of respired CO₂ by the anaplerotic pathway, involving the PEPC and generating ¹³C-enriched organic acids due to the fractionation in favour of ¹³C, with discrimination relative to gaseous CO₂ of about -5.7 ‰, including therefore those of the carbonic anhydrase (CA) involved in the hydration of CO₂ (respectively 2.2 ‰ discrimination for the PEPC and -9 ‰ for the CA, Badeck *et al.* 2005; Ghashghaie and Badeck 2014).

Our objective was to clarify which carbon sources contribute to the fast-growing stage of immature culms of *P. edulis*, from the developing culm itself or exogenously from mature bamboos. We postulated that photosynthates produced by the mature bamboos are the main carbon source for the fast growth of developing bamboo culm and that, therefore, the δ¹³C of developing bamboo does not strongly differ from the δ¹³C of all organs of mature *P. edulis*. To test this

hypothesis, we collected samples of various organs at both the autotrophic and heterotrophic stages and analysed their natural ¹³C abundance in the bulk organic matter and the fractions of different organic compounds. We further postulate that developing culms can nevertheless fix a limited amount of CO₂ during the FGP. To test this hypothesis, we operated a ¹³C pulse labelling at the surface and in the hollow of the developing culm and traced the labelled carbon in the soluble polar fraction (sugars, amino acids and organic acids) in the tissues of the developing culms.

Materials and Methods

Experimental site

This study was conducted in a moso bamboo stand at the Katsura Campus, Kyoto University (Kyoto Prefecture, Japan; 34°59′06.2″N, 135°40′48.4″E, 110 m alt.). Mean annual temperature and mean annual precipitation in 2021 were 16.9 °C and 1552 mm. The stand management included rough selective cutting and bamboo shoot harvesting without fertilisation. The mean height of the culms of mature bamboos was 15.3 m and the average diameter at breast height (DBH) was 9.9 cm.

Sample collection of isotope analysis (natural abundance)

Between April and May 2021, three replicates of each organ were collected from three different individuals, including culms, branches, leaves, rhizomes and roots for mature bamboos; and bamboo shoots and developing culms for developing bamboos (Fig. 1). Samples were frozen in liquid nitrogen and first stored at -15 °C in a portable freezer in the field before being transferred to -20 °C in the laboratory.

¹³CO₂ labelling experiment

The ¹³CO₂ pulse labelling experiment was conducted on 11 May 2021. Six immature, leafless but vigorous culms of similar size were selected (mean DBH = 11.7 cm, mean height = 6 m). Three labelling chambers were installed on three developing culms around the 7th internode from the ground without sheaths (chamber size, Φ = 20 cm, height = 15 cm). The chambers were made of a transparent thin polycarbonate sheet wrapped around the culm on polypropylene half-circular plates at both the bottom and the top of the chamber, with semi-circular holes at their centre to accommodate the culm. They were affixed to the surface of the culm with neutral seal putty and a silicon sealant [see Supporting Information—Fig. S1]. At 13:20 h, 75 mL of 99 % ¹³CO₂ was injected into each chamber from three directions (three times 25 mL with a needle inserted through the polycarbonate sheet). The concentration of ¹³CO₂ in the chambers was 2.4 ‰, based on the volume of the chamber and the amount of ¹³CO₂ injected. In the other three developing culms, 50 mL of 99 % ¹³CO₂ was injected with a needle inserted into the hollow of the 7th internode without sheaths. The concentration of ¹³CO₂ in the hollows was 3.7 ‰, based on the volume of the hollow and the amount of ¹³CO₂ injected. The small pinhole was sealed by tape. Two hours after the injection of ¹³CO₂ in either the chamber or the culm hollow, the 5th, 7th and 9th internodes of the six labelled and two unlabelled developing culms were sampled. Disks of 100–200 g were collected using a hand saw shortly after labelling to limit the

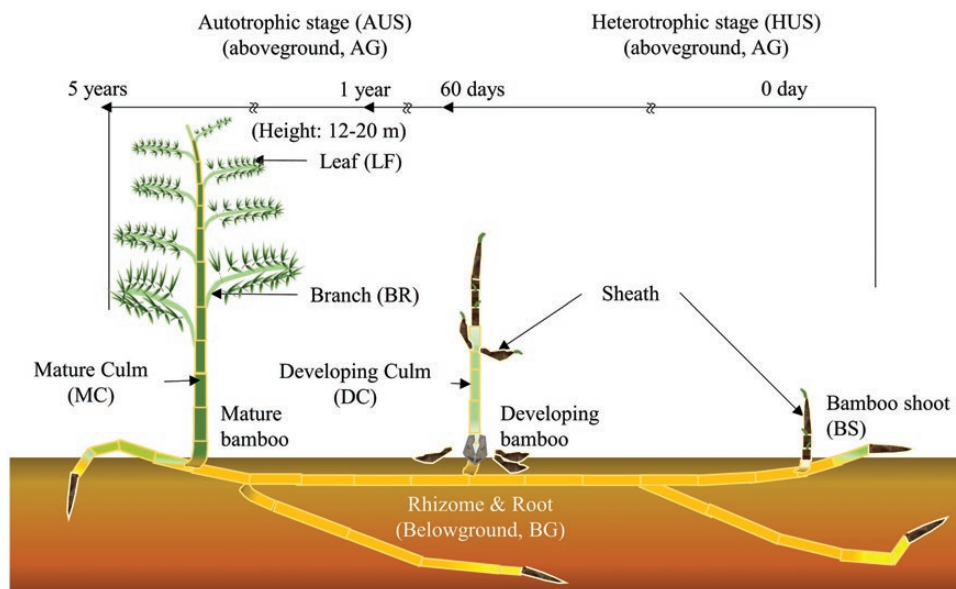


Figure 1. Illustrations of *P. edulis* at different growth stages. Mature bamboo culms (MC) (autotrophic stage, AUS) bear branches (BR) and leaves (LF) (aboveground, AG) and rhizomes (RH) and roots (RO) in the soil (belowground, BG). Young bamboo shoots (BS) emerge from the ground attached to mature bamboo rhizomes. Developing, immature culms grow rapidly within 3 months (heterotrophic stage, HES). Young bamboo shoots are shoots covered by sheaths before the internodes undergoing extensive elongation. Developing culms are the growing culms that undergo a period of rapid internode elongation, after which the senescence of the sheath occurs, and eventually mature into fully formed culms.

proportion of labelled products potentially transported away from the assimilation site. Samples were frozen in liquid nitrogen and first stored at $-15\text{ }^{\circ}\text{C}$ in a portable freezer in the field before being transferred to $-20\text{ }^{\circ}\text{C}$ in the laboratory, as above.

Purification of polar fractions, structural compounds, starch and proteins from different organs

In the laboratory, all samples were freeze-dried for at least 72 h using a vacuum freeze dryer (FDU-1200, EYELA, Tokyo, Japan), and ground to a fine powder in a ball mill (MM-400, Retsch, Düsseldorf, Germany).

The polar fraction, starch, proteins and structural compounds were separated and purified according to the modified methods of Deleens and Garnier-Dardart (1977), Wanek *et al.* (2001), Richter *et al.* (2009) and Desalme *et al.* (2017). These purification procedures have been developed specifically to allow the carbon isotope analysis of organic fractions. Briefly, soluble and insoluble compounds were separated based on their polar properties in a mixture of methanol–chloroform–water (12/5/3, v/v/v). After centrifugation, the supernatant was mixed with 0.5 mL of methanol–chloroform (MC, 1/1, v/v) to separate pigments and lipids in the lower phase from the polar compounds in the upper phase. The pellet was digested with pronase in Tris buffer. Proteins were solubilised while starch remains in the insoluble fraction. The insoluble fraction was washed with ethanol and starch was gelatinised by hydrochloric acid. The starch fraction, recovered in the supernatant after centrifugation, was precipitated with absolute methanol. The structural fraction was recovered in the pellet washed with water at least 3 times. All fractions were oven-dried at $65\text{ }^{\circ}\text{C}$ and weighed. The methodology detailed step by step is available [see Supporting Information—Method S2 and Fig. S2].

$\delta^{13}\text{C}$ determination of total organic matter, polar fractions, structural compounds, starch and proteins

For the determination of the isotope composition, 1 mg of dried samples or dried fractions was weighed in tin capsules and combusted in elemental analysers coupled to isotope ratio mass spectrometers (Thermo FLASH2000, DeltaV advantage with ConFloIV system, Thermo Fisher Scientific, Massachusetts, USA; for unlabelled samples, and Thermo NC2500, MAT252 with ConFloIII system, Thermo Fisher Scientific, Massachusetts, USA; for labelled samples). Several international standards [IAEA-CH-3 ($-24.724\text{ }^{\circ}\text{‰}$, Coplen *et al.* 2006), USGS40 ($-26.39\text{ }^{\circ}\text{‰}$, Qi *et al.* 2003) and USGS41a ($36.55\text{ }^{\circ}\text{‰}$, Qi *et al.* 2016)] were used for calibrations. USGS 41a was further used as a running standard for every 11 samples. The analysis of the 11 samples would have been rerun if the running standard had been an outlier of all standards (outlier defined in Reed *et al.* 1971), which did not happen. Results ($\delta^{13}\text{C}$) were expressed in ‰ as the relative deviation of the isotope ratio of the sample ($^{13}\text{C}/^{12}\text{C}$, R_{sample}) compared to that of the international VPDB standard (Vienna PeeDee Belemnite).

$$\delta^{13}\text{C} = \left(\frac{R_{\text{sample}}}{R_{\text{vpdb}}} - 1 \right) \quad (1)$$

The isotope composition of the weighted fractions ($\delta^{13}\text{C}_{\text{all}}$) was defined as:

$$\delta^{13}\text{C}_{\text{all}} = \frac{\sum \delta^{13}\text{C} \times C_f \times W_f}{\sum C_f \times W_f} \quad (2)$$

with C_f , the carbon ratio for each fraction refers from Bowling *et al.* (2008), and W_f , the dry weight of fraction.

The excess amount of ^{13}C in a labelled sample was calculated as:

$$\text{Excess}^{13}\text{C} = \left(x(^{13}\text{C})_{\text{L}} - x(^{13}\text{C})_{\text{UN}} \right) \times C \quad (3)$$

with $x(^{13}\text{C})_{\text{L}}$ and $x(^{13}\text{C})_{\text{UN}}$, the atom fraction of ^{13}C in labelled and unlabelled samples respectively, and C, the total carbon content.

The atom fraction was calculated as:

$$x(^{13}\text{C}) = \frac{^{13}\text{C}}{^{12}\text{C} + ^{13}\text{C}} = \frac{R_{\text{sample}}}{R_{\text{sample}} + 1} \quad (4)$$

Culm anatomy and starch granule observation

The 7th internode of developing culms was cut into small cubes. Cross and vertical sections 10–30 μm thick were sliced off the frozen samples (MCR802A, Komatsu Electronics, Ishikawa, Japan) with a sliding microtome (TU-213, Yamato Kohki, Saitama, Japan). Each section was loaded on a glass slide and covered carefully with a coverslip to avoid air bubbles. After initial observation, sections were rinsed with ultrapure water and stained with 0.1 N iodine solution, and briefly rinsed with ultrapure water again. Microphotograph images were taken with a digital camera (EOS KISS X3, Canon, Tokyo, Japan) attached to a light microscope (13X50-32, Olympus, Tokyo, Japan).

Chlorophyll content measurement

Two mm wide vertical sections of the skin, middle and inner parts of the 7th internode in developing culms were cut for chlorophyll extraction. Chlorophyll was extracted from 500 mg of fresh samples using 4 mL of *N,N*-dimethylformamide as the extraction solvent. Extraction was conducted in darkness at 65 $^{\circ}\text{C}$ for 2 h followed by 1 h at room temperature (Berveiller and Damesin 2008). At the end of the extraction, the samples were colourless. The absorbance of the extract was measured at 470, 663.6 and 646.6 nm using a spectrophotometer (ASV-S3, As One Corporation, Osaka, Japan). The amounts of chlorophyll *a* and *b* were calculated using the extinction coefficients obtained from Porra *et al.* (1989).

Statistical analysis

Data presented in this study are the means of three replicates from three individuals. One-way ANOVA followed by the Tukey HSD post hoc test was performed to test the between-organ differences in $\delta^{13}\text{C}$ in bulk organic matter and in different organic fractions, and the content in these different fractions. It was also used to test the differences in chlorophyll content between the skin, middle and inner tissues of the developing culms. Univariate student's *t*-test was used to test whether the excess ^{13}C in the polar fraction was significantly higher than 0 after pulse-labelling developing culms with $^{13}\text{CO}_2$. All statistical analyses were performed using R (R Core Team 2023).

Results

Variations in natural ^{13}C abundance in bulk organic matter between organs

The isotope composition of the different autotrophic organs of mature bamboos (leaves and branches) and belowground systems (rhizomes and roots) ranged between -28.4 and -30.2 ‰ (-29.3 ‰ on average, Fig. 2). The isotope composition of culms was higher than that of mature bamboo branches and leaves (-28.5 and -29.8 ‰ on average, respectively; $P < 0.05$; Fig. 2). The bulk $\delta^{13}\text{C}$ of bamboo shoots and developing culms (-26.8 and -26.3 ‰ on average; Fig.

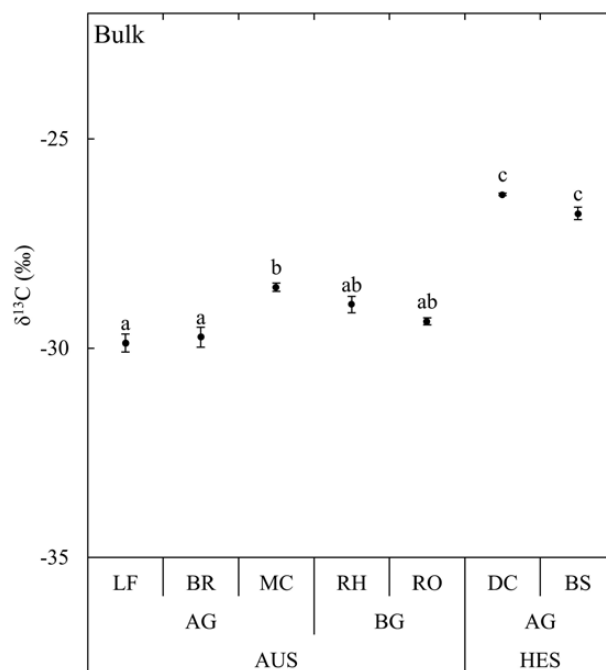


Figure 2. Isotope composition ($\delta^{13}\text{C}$) of bulk organic matter in organs of *P. edulis* at different growth stages. Average ($n = 3$) with standard errors are shown. Different letters indicate significant differences (one-way ANOVA and Tukey HSD post hoc test at $P < 0.05$) between leaves (LF), branches (BR), mature culms (MC), rhizomes (RH), roots (RO), developing culms (DC) and bamboo shoots (BS). The autotrophic stage (AUS) includes both aboveground (AG) and belowground (BG) organs of mature bamboos. The heterotrophic stage (HES) includes newly formed bamboo shoots and developing immature bamboo culms during their fast-growing period (FGP).

2) were higher than that of all organs of mature bamboos ($P < 0.001$).

Variations in the content of biochemical fractions between organs

The content in the polar fraction was higher in the foliage than in other organs of mature bamboo and developing immature bamboo shoots ($P < 0.001$) but similar to that in young bamboo shoots ($P > 0.05$; Fig. 3A). The starch content was low in all organs, especially in the belowground part of the mature bamboos, except in the young bamboo shoots (Fig. 3B). More proteins were found in the aboveground organs of mature bamboos than in their belowground organs. While the protein content was not different in developing bamboo culms compared to mature bamboos ($P > 0.1$), the young bamboo shoots contained a much larger amount of proteins than all the other samples (0.48 g g^{-1} compared to 0.09 g g^{-1} on average in all other samples; $P < 0.001$; Fig. 3C). The content in structural compounds was much lower in young bamboo shoots (0.10 g g^{-1} ; $P < 0.001$; Fig. 3D) than in all the other organs. Low values were also observed in leaves (0.55 g g^{-1} , Fig. 3D), while it averaged 0.84 g g^{-1} in the belowground organs, 0.75 g g^{-1} in branches and mature culm and 0.70 g g^{-1} in developing bamboo culms (Fig. 3D).

Variations in natural ^{13}C abundance between biochemical fractions

The polar fraction was depleted in ^{13}C compared to the bulk organic matter and showed large variations among organs,

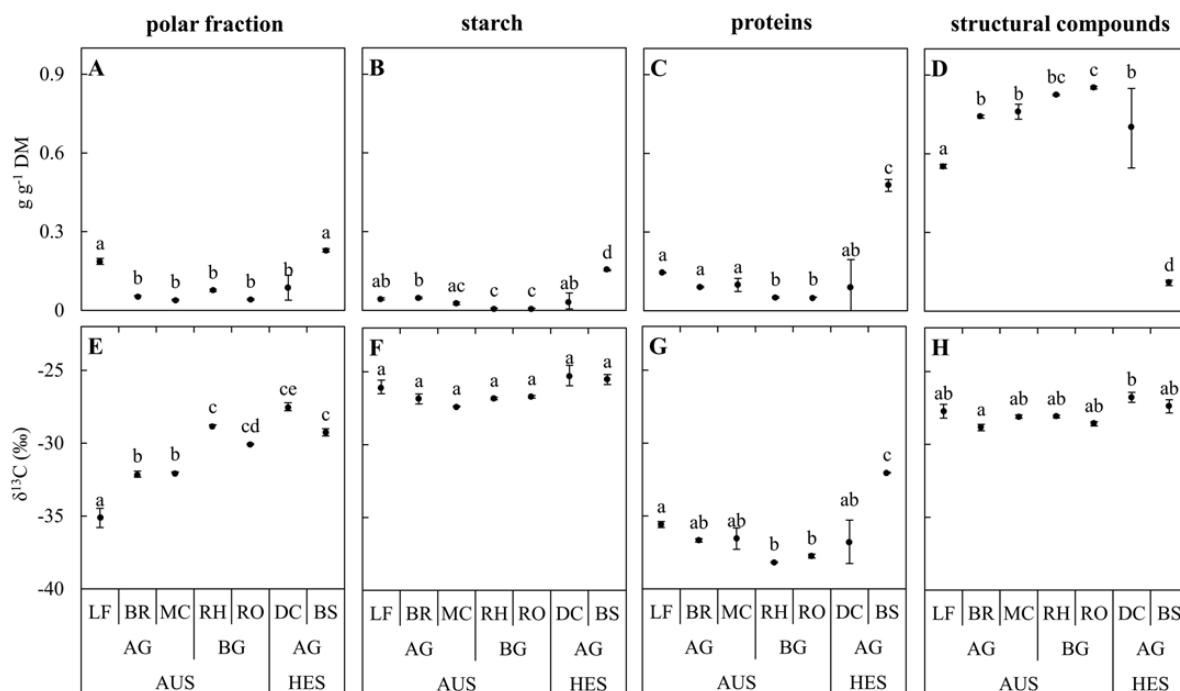


Figure 3. Contents and isotope carbon compositions ($\delta^{13}\text{C}$) of main biochemical fractions in organs at different growth stages. (A and E) Polar fraction. (B and F) Starch. (C and G) Proteins. (D and H) Structural compounds. Average ($n = 3$) with standard errors are shown. Different letters indicate significant differences among organs (one-way ANOVA and Tukey HSD post hoc test at $P < 0.05$). LF, BR, MC, RH, RO, DC and BS indicate leaves, branches, mature culms, rhizomes, roots, developing culms and bamboo shoots, respectively. The autotrophic stage (AUS) includes both aboveground (AG) and belowground (BG) organs of mature bamboos. The heterotrophic stage (HES) includes newly formed bamboo shoots and developing immature bamboo culms during their fast-growing period (FGP).

from -35.1 ‰ in leaves to -27.5 ‰ in developing bamboo culms (Fig. 3E). The isotope composition of polar fractions from the rhizome (-28.8 ‰), less depleted than that of the other organs of the mature bamboos (< -30 ‰), was not different than that of the developing bamboo culms (-27.5 ‰; $p > 0.1$) and young bamboo shoots (-29.3 ‰; $P > 0.1$). In contrast to the polar fraction, the starch fraction was enriched in ^{13}C compared to the bulk organic matter and much less variable (Fig. 3F). The protein fraction was strongly depleted in all organs compared to the bulk organic matter (from -35.6 to -38.2 ‰, Fig. 3G) except for the young bamboo shoots, which showed a $\delta^{13}\text{C}$ higher value than that of all other organs (-32.0 ‰; $P < 0.001$). $\delta^{13}\text{C}$ of the structural compounds was slightly higher in the developing bamboo culm (-26.6 ‰, Fig. 3H) than that of the organs of mature bamboos (< -27.7 ‰).

The weighted average of the isotopic composition of the different biochemical fractions (polar fractions, starch, proteins and structural compounds) by their concentration and carbon content ($\delta^{13}\text{C}_{\text{all}}$) was compared to the isotope composition of the bulk organic matter ($\delta^{13}\text{C}_{\text{bulk}}$), and the deviation can be attributed to the isotope composition of unknown compounds, especially lipids and other non-polar molecules, which have been solubilised in chloroform but not analysed isotopically due to their limited quantity. No pronounced differences between $\delta^{13}\text{C}_{\text{bulk}}$ and $\delta^{13}\text{C}_{\text{all}}$ were observed in mature organs (leaves, branches and culms) and belowground systems (rhizomes and roots). However, bulk organic matter in developing bamboo culms and young bamboo shoots was more enriched in ^{13}C than the analysed compounds (Fig. 4).

Chlorophyll content and anatomy of developing culms at the 7th internode

The chlorophyll content in the skin of developing culms, which includes the layer of cortical cells, was higher than in middle and inner tissues ($26.1 \mu\text{g g}^{-1}$ FW compared to 4.4 and $0.5 \mu\text{g g}^{-1}$ FW on average, respectively; $P < 0.001$; Fig. 5A). However, when expressed per unit area, the chlorophyll content in the skin was similar to that in mature leaves (respectively 5.6 and $4.2 \mu\text{g cm}^{-2}$ on average). Chlorenchyma cells were distributed around the skin of developing culms (Fig. 5C–E). In the middle part of the developing culm, chlorophyll was found preferentially near the metaxylem vessels and the phloem sieve tubes forming a bundle sheath around the vascular bundles (Fig. 5F and G). Furthermore, a lot of starch granules were observed in parenchyma cells around the vascular bundles of developing culms. In contrast, almost no starch granules were observed in the parenchyma cells of the inner part and the chlorenchyma cells of the skin part of developing culms (Fig. 5H and I).

Distribution of labelled carbon after ^{13}C pulse labelling of the 7th internode of developing culms

The excess ^{13}C of the polar fraction (PF) extracted from the 7th internode of developing culms was significantly higher than 0 near the skin ($0.1 \text{ mg } ^{13}\text{C g}^{-1}$ PF on average, Fig. 6A) while it was not significantly different from 0 deeper in the culms ($0.0003 \text{ mg } ^{13}\text{C g}^{-1}$ PF in the middle and $0.001 \text{ mg } ^{13}\text{C g}^{-1}$ PF in the inner parts on average). When $^{13}\text{CO}_2$ was injected in the hollow inside the 7th internode of the developing culms, little or no enrichment was recovered in any sample

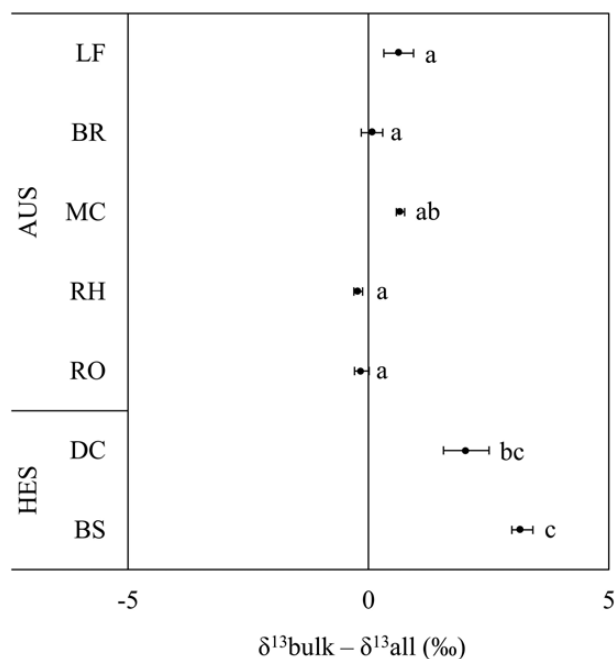


Figure 4. Deviation between the weighted average of the isotopic composition of the different biochemical fractions ($\delta^{13}\text{all}$) and the isotope composition of the bulk organic matter ($\delta^{13}\text{bulk}$). $\delta^{13}\text{all}$ is the weighted average of the isotopic composition of the different biochemical fractions (polar fractions, starch, proteins and structural compounds) by their concentration and carbon content. Average ($n = 3$) with standard errors are shown. Different letters indicate significant differences among organs (one-way ANOVA and Tukey HSD post hoc test at $P < 0.05$). LF, BR, MC, RH, RO, DC and BS indicate leaves, branches, mature culms, rhizomes, roots, developing culms and bamboo shoots, respectively. The autotrophic stage (AUS) includes both aboveground (AG) and belowground (BG) organs of mature bamboos. The heterotrophic stage (HES) includes newly formed bamboo shoots and developing immature bamboo culms during their fast-growing period (FGP).

compared to unlabelled samples, but it was significantly different from 0 in the inner part, although the enrichment value was small ($0.002 \text{ mg } ^{13}\text{C g}^{-1} \text{ PF}$, Fig. 6B). No enrichment was found in the internodes below (5th) or above (9th) the internode 7th which was labelled, confirming that the labelled carbon did not migrate up or down during the short 2-h tracing (data not shown).

Discussion

Only slight ^{13}C enrichment of heterotrophic organs compared to leaves

The isotope composition of the different autotrophic organs of mature bamboos (Fig. 2) was similar to those of mature leaves in a previous study (-28.3 ‰ , Hanba *et al.* 2010), confirming that *P. edulis* is a C_3 plant at the autotrophic stage. The slight enrichment in ^{13}C of the different heterotrophic organs of mature bamboo (culms, rhizomes and roots) compared to autotrophic organs agrees with previous findings in several studies summarised by Badeck *et al.* (2005): roots, stems or culms (grass stems) are often slightly enriched in ^{13}C compared to leaves (1–2 ‰). The reasons for this phenomenon, which is often related to post-photosynthetic fractionations, are complex, and several hypotheses have been reviewed by Cernusak *et al.* (2009). Since the isotopic composition

of starch was similar for all organs while differences were found for other fractions, a seasonal change in ^{13}C discrimination during photosynthesis (their hypothesis 2) or preferentially nocturnal sucrose translocation (their hypothesis 3) are therefore unlikely to explain the ^{13}C enrichment of immature bamboo and heterotrophic organs of mature bamboo compared to leaves. Heterogeneous carbon isotope distribution within sugars results from enzyme-dependent fractionations occurring during sugar interconversions. Because these sugars are precursors of all organic compounds in plant tissues, these fractionations impact the ^{13}C distribution in plants (Rossmann *et al.* 1991; Gilbert *et al.* 2012), given that different types of biochemical substances do not have the same isotope characteristics (Bowling *et al.* 2008). The differences in the isotope composition between organs are therefore thought to be related to their differences in the biochemical composition (Cernusak *et al.* 2009, their hypothesis 1). However, although different biosynthetic pathways cause carbon-related compounds in different organs to have different ^{13}C , the remaining part of the biosynthesis of a certain compound is used in the biosynthesis of other compounds, so the bulk $\delta^{13}\text{C}$ of the organ should not be determined by internal compounds but by the balance between carbon input and output (Badeck *et al.* 2005; Gilbert *et al.* 2012). The fact that the assimilates transported from the leaves to the remaining part of the plant (input) are enriched in ^{13}C due to post-photosynthetic fractionations associated with mitochondrial respiration occurring in the leaves (Damesin and Lelarge 2003; Gessler *et al.* 2007; Kodama *et al.* 2008) can therefore explain the observed slight enrichment of these heterotrophic organs (Cernusak *et al.* 2009, their hypothesis 4). Also, additional fractionations related to incomplete decarboxylation during respiration (output) can release depleted CO_2 and contribute to the enrichment of the remaining organic matter (Damesin and Lelarge 2003; Ghashghaie and Badeck 2014). The fact that the polar fraction was similarly enriched in the belowground organs of mature bamboos and in the bamboo shoots and developing culms compared to the autotrophic organs of mature bamboos supports the hypothesis that photosynthates produced by the mature bamboos and stored in the rhizome are the main carbon source for the fast growth of developing bamboo culm (Fig. 3E). This is also consistent with the fact that the starch content was very low in the belowground part of the mature bamboos, but high in the young bamboo shoots, which may have temporarily stored starch just before the onset of the FGP (Fig. 3B). The fact that the isotopic composition of starch from young shoots was similar to that of starch from leaves of mature bamboos (Fig. 3F) suggests a possible common sugar source.

It has been shown in another bamboo (*Phyllostachys nigra*) that the chemical composition of the cell wall changed with time and that lignin accumulated at a later stage of development (Chang *et al.* 2013). It is therefore possible that the lower $\delta^{13}\text{C}$ values in mature bamboo culms are related to a high proportion of lignin in their structural fraction compared to immature bamboos. Lignin is indeed depleted in ^{13}C compared to cellulose or other structural polysaccharides (Bowling *et al.* 2008) because lignin precursors are produced by the shikimate pathway, which is fuelled by the depleted products of the pyruvate dehydrogenase and the Krebs cycle (Gessler *et al.* 2014). However, the isotope composition of the structural compounds was very similar in developing culms, bamboo shoots and organs of mature bamboos (Fig. 3H). It

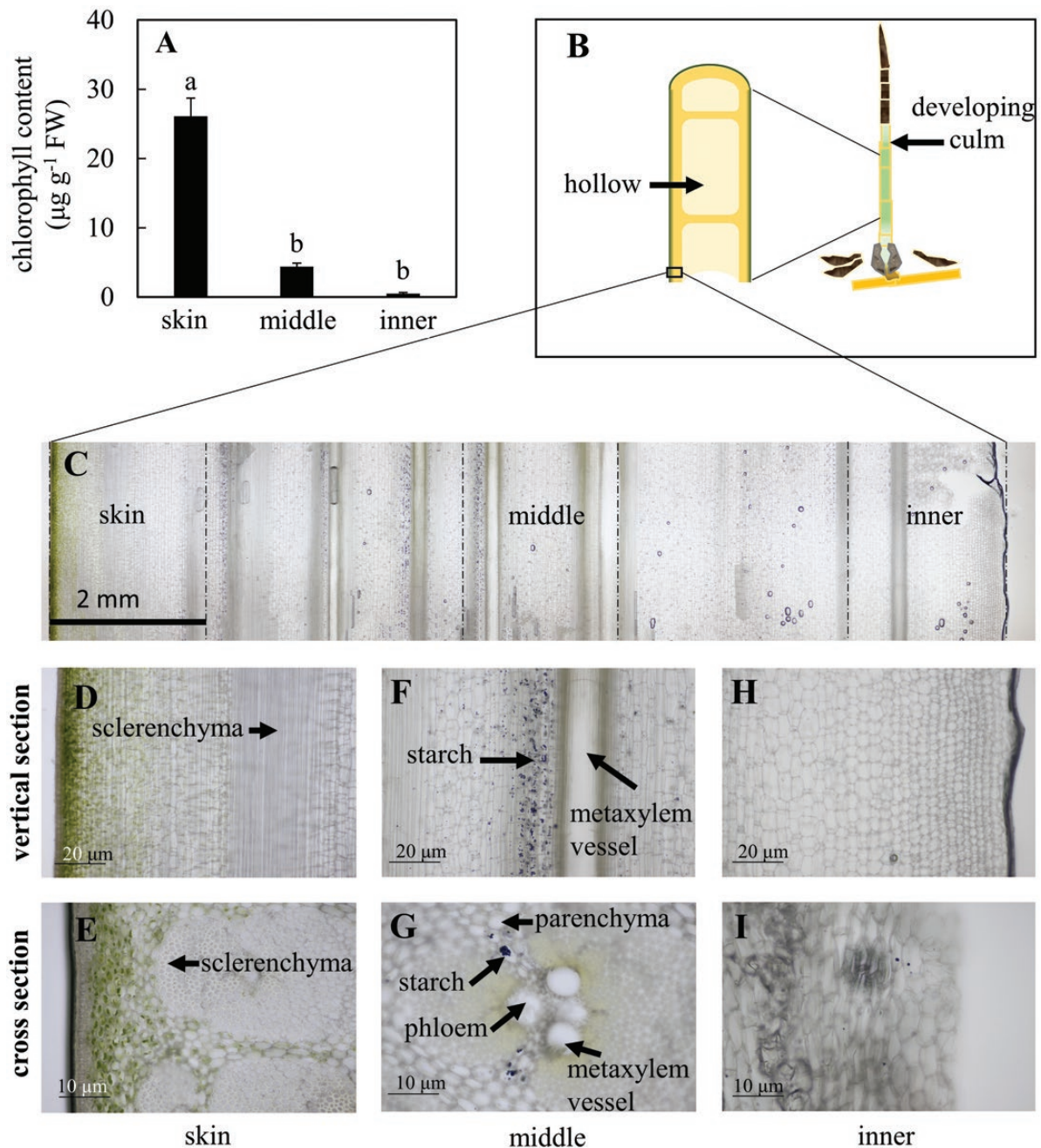


Figure 5. Chlorophyll content and anatomy of developing culms. (A) Average chlorophyll content with their standard errors ($n = 6$) in developing culm at different radial positions. Different letters indicate significant differences (one-way ANOVA and Tukey HSD post hoc test at $P < 0.05$). (B) Illustration of a developing culm with its internal hollow. (C) Vertical section of developing bamboo culm. (D) Vertical section of skin tissues. (E), Cross-section of the skin tissues. (F) Vertical section of tissues in the middle. (G) Cross-section of tissues in the middle. (H) Vertical section of the inner tissues. (I) Cross-section of the inner tissues.

is therefore unlikely that the observed depletion of mature culms relative to the immature ones was related to lignin accumulation with ageing.

Photosynthesis in new-born bamboo culms during the FGP

Huge amounts of carbohydrates should be either produced or transported from mature bamboos to meet the high demand needed to support cell elongation in the internodes of the immature bamboo culms during the period of rapid growth. Using ¹³C-enriched CO₂ labelling, we found direct evidence

that the skin of developing culm slightly uptakes the CO₂ from the atmosphere and synthesises carbohydrates (Fig. 6A). However, because the concentration of CO₂ in the labelling chamber was much higher than in the atmosphere (2.4 %), our results revealed a potential rather than the actual CO₂ fixation. In addition, the estimated rate of CO₂ fixation by the immature culms based on excess ¹³C in the polar fraction, which was about 0.1 µmol m⁻² s⁻¹, was more than 100 times lower than expected leaf photosynthesis (Zachariah *et al.* 2016) and 20 times lower than the respiration of young culms (Uchida *et al.* 2022). Our results are therefore consistent with

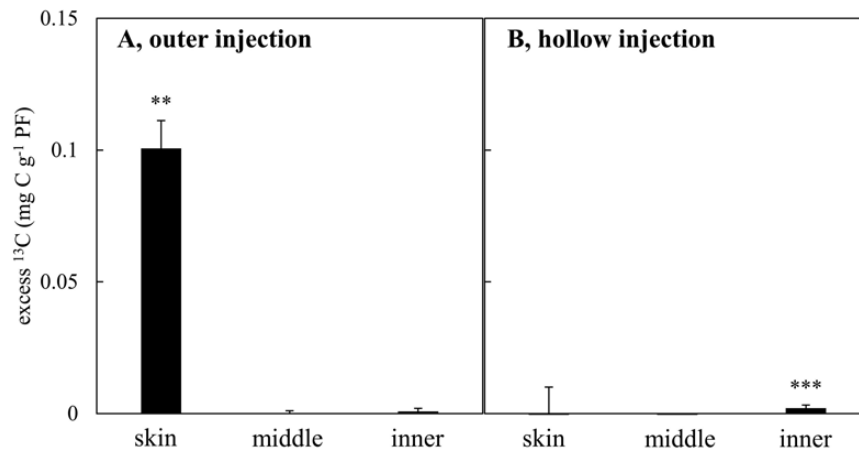


Figure 6. Excess ^{13}C in after a pulse $^{13}\text{CO}_2$ labelling at the 7th internode of developing culms during the fast-growing period. Average with their standard error ($n = 3$) of excess ^{13}C in the polar fraction (PF) extracted from the skin, middle and inner tissues of the developing culms 2 h after the injection of $^{13}\text{CO}_2$ in either a chamber around the culm (left, A) or the culm hollow (right, B). '****' and '***' indicate that the average excess ^{13}C is greater than 0 (univariate student's t -test at $P < 0.001$ and $P < 0.01$).

the low chlorophyll content in the skin of developing culms compared to leaves (Fig. 5A) and the observed translocation of photosynthates from mother to daughter ramets of moso bamboo quantified using ^{13}C - CO_2 pulse labelling (Zhai *et al.* 2022).

Previous studies have also pointed out that the developing culms of *P. edulis* activated the key enzymes of C_4 carbon fixation (such as NADP-ME, NADP-MDH, pyruvate phosphate dikinase [PPDK] and PEPC) during the FGP (Wang *et al.* 2012, 2021). A C_4 plant-like Kranz anatomy has also been evident in the middle of the developing bamboo culm in this study (Fig. 5F and G), confirming previous observations (Wang *et al.* 2012). Another hypothesis to explain the slight enrichment of the bamboo shoots and developing culms is therefore that the PEPC is involved in a limited carbon fixation by immature culms during their initial growth, like C_3 - C_4 intermediate species (Lundgren *et al.* 2016). PEPC refixation may contribute with malate to the Krebs cycle, thus resulting in ^{13}C -enriched respired CO_2 (Cernusak *et al.* 2009, their hypothesis 5; Gessler *et al.* 2009). However, based on direct evidence from our $^{13}\text{CO}_2$ pulse labelling, the assimilation of atmospheric CO_2 seems to be limited to the skin of the culm, as only the tissue near the skin was labelled when $^{13}\text{CO}_2$ was provided around the culm, while the C_4 plant-like Kranz anatomy was found in the middle part of the culm. In addition, the isotope composition of the starch in developing culms and bamboos shoots was not different than that in any organ of mature bamboos, which definitely excludes significant C_4 -like photosynthetic carbon fixation in immature culms (Fig. 3F).

The presence of a limited amount of chlorophyll and a large number of starch granules in the parenchyma cells around the vascular bundle in the middle part of the culm nevertheless suggests that CO_2 assimilation can occur, the CO_2 being potentially supplied by the xylem sap rather than diffusing from the atmosphere or the internal hollow because of limited diffusion of CO_2 within the dense culm tissues. A high amount of water flows through the rhizome to supply the fast-growing shoots and culms with water and nutrients (Zhang *et al.* 2020). Berveiller & Damesin (2008) found that the activities of PEPC and NADP-ME were up to 13 and 30 times higher in stems than in leaves of European beech. High PEPC

activity can supply malate to the NADP-ME enzyme which, in turn, can supply CO_2 for Rubisco after decarboxylation, recycling CO_2 derived internally from respiration, as it was postulated in stems of tobacco, celery and mikania that have characteristics of C_4 photosynthesis in stems and exhibited a C_4 plant-like Kranz anatomy (Hibberd and Quick 2002). However, it remains unclear whether enough light can reach the photosynthetic pigments in the bundle sheath and provide enough energy to sustain a C_4 -like carbon fixation under the deep shade conditions that prevail in the understory of a *P. edulis* because the C_4 photosynthesis became unfavourable at low PPFD (Bellasio and Farquhar 2019). In addition, the starch in the numerous granules should have been enriched compared with CO_2 derived from the oxidation of imported sugars if a large fraction of respired CO_2 was reassimilated by the PEPC and used in gluconeogenesis. This is because the fractionation in favour of ^{13}C by the CA involved in the hydration of CO_2 is higher than the small fractionation against ^{13}C by the PEPC (Badeck *et al.* 2005; Ghashghaie and Badeck 2014). Such enrichment was not observed in starch (Fig. 3F), suggesting that the abundant recycled CO_2 was not used for starch synthesis but for other purposes. This again suggests that the starch was instead likely synthesised from sucrose produced in mature bamboo, transported in the phloem through the rhizomes and transiently stored in granules near elongating cells (Li *et al.* 2022). On the other hand, carbon derived from the breakdown of stored starch in mature bamboo organs should be ^{13}C -enriched, as compared to primary assimilates, because starch breakdown produced ^{13}C -enriched sucrose (Gessler *et al.* 2008). Therefore, a higher contribution of stored carbon to boost developing culms may lead to enriched ^{13}C organic matter in immature culms.

Anaplerotic fixation of respired CO_2 in immature bamboo culms during the fast growth period

The inner part of the culm was slightly labelled when $^{13}\text{CO}_2$ was provided in the culm hollow (Fig. 6B). This may reveal that carbon fixation is taking place in the inner parts. It has been shown that carbon fixation by the PEPC can occur in darkness in some tree stems (Höll 1974; Langenfeld-Heyser 1989) and can be stimulated in the presence of nitrate and

ammonium (Müller *et al.* 1991; Vuorinen and Kaiser 1997). The CO₂ concentration inside culms of moso bamboos, which varies during the day and over the season from 40 000 to more than 100 000 ppm (Toshihiko Maitani, unpublished results), is in a similar range as for other bamboo species (Kiyama 1905; Zachariah *et al.* 2016). Therefore, it is also possible that PEPC and NADP-ME are involved in the anaplerotic fixation of respired CO₂ in the middle and inner culms where light cannot reach, providing the carbon skeleton (malate and oxaloacetate) necessary for amino-acid (Berveiller and Damesin 2008) and lipid syntheses (Smith *et al.* 1992), which are also needed during the FGP of bamboo. As explained above, because the fractionation in favour of ¹³C by the CA involved in the hydration of CO₂ is higher than the small fractionation against ¹³C by the PEPC, the organic acids issued from the anaplerotic pathway are expected to be enriched. The discrepancy between δ¹³bulk and δ¹³all (weighted average of the isotopic composition of the four biochemical fractions analysed) in developing bamboo culms and young bamboo shoots (Fig. 4), which can be attributed to the isotope composition of lipids and other non-polar molecules as mentioned above, suggests that ¹³C-enriched malate, involved in the fatty acid synthesis, is partly derived from the anaplerotic fixation of CO₂. The impact of the anaplerotic dark CO₂ fixation on the enrichment of plant tissues also depends on how much respired CO₂ can be reassimilated (Nalborczyk 1978). The use of ¹³C-enriched organic acids issued from the anaplerotic pathway for nitrogen assimilation may explain the slight enrichment of the abundant proteins extracted from bamboo shoots, and why this enrichment starts to vanish when the new culm is developing (Fig. 3G). While most nitrogen needed to support the fast growth is potentially remobilised from the mature bamboos and transferred via the rhizome (Shi *et al.* 2021, 2022; Zhai *et al.* 2022), additional nitrogen assimilation can occur.

Conclusions

In spring, the bamboo shoots emerge, and the developing bamboos enter a phase of active and very rapid growth. Because the leaf of new-born bamboo had not yet developed, the main sources of carbohydrates during the FGP were supplied by mature bamboos and delivered through their belowground system to the developing culms, which is consistent with a slight ¹³C enrichment of the bulk organic matter of immature bamboos. Although previous studies observed key enzymes related to C₄ carbon fixation, the results based on ¹³C pulse labelling showed limited CO₂ uptake from the atmosphere and hollow during the FGP. Limited anaplerotic dark fixation of CO₂ is more likely to occur than C₄ photosynthetic C fixation.

Supporting Information

The following additional information is available in the online version of this article –

Figure S1. Schematic illustration of ¹³CO₂ labelling in developing culms of *Phyllostachys edulis*.

Methods S2. Procedure of purification for the polar fraction, structural compounds, starch and proteins from different organs in plants adjusted for *P. edulis*.

Figure S2. Flow chart of the laboratory analytical procedure for carbon compound purification in plant samples.

Funding

This work was supported by JSPS KAKENHI Grant Numbers JP15H04513, JP19J11336 and JP20J15519. The authors declare that they have no competing financial interests or personal relationships that could have influenced the work reported in this paper.

Conflict of Interest Statement

None declared.

Acknowledgements

The authors are grateful to professor Y. Kosugi for searching the study site, to Dr T. Tanabe, Mr R. Fujii, Mr S. Paul, Mr K. Hayashi and Mr T. Mochitome for their help in the field and fruitful discussion, to retired professor N. Okada and Mr Aye Ko Ko for their advice on preparing and imaging micro-sections for anatomy, to Ms S. Tsuji and Ms C. Tsuji for their advice on purifying for carbon compounds, to retired professor W. Liese and professor J. Ghashghaie for sharing their precious studies which are not available on the internet, to retired professor A. Osawa, Ms M. Watanabe, Ms N. Shiozaki, Ms M. Fukuda, Ms E. Kita, Dr H. Kajino, professor K. Kitajima, professor Y. Onoda, retired professor K. Kitayama, Dr A. Kagawa, retired professor A. Osawa for environmental support, to Dr H. Schäfer, Ms Y. Kihara, Ms Y. Xia, Mr Y. Sawada, Ms E. Nishitsuji, Dr B. A. T. M. Zinnatul, professor A. Katayama, professor T. Kume, professor Y. Isagi, professor S. Shibata, Dr T. H. Chen and Dr M. Watanabe for discussion, to Dr J. Pinos, Ms A. Amariei, Mr L. Butkus, Mr A. Pabedinskas, Ms N. Tabaja, and all members in Forest Utilisation lab at Kyoto University and in 2019 SIFER International Doctoral Course at Institut national de la recherche agronomique for conceptualisation.

Data Availability

The data underlying this article are available in the Dryad repository at <https://doi.org/10.5061/dryad.brw15dvf9>, and the newest version of data will be updated in the Open Science Framework (OSF) repository, at <https://doi.org/10.17605/OSF.IO/AVPKN>

References

- Badeck FW, Tcherkez G, Nogués S, Piel C, Ghashghaie J. 2005. Post-photosynthetic fractionation of stable carbon isotopes between plant organs—a widespread phenomenon. *Rapid Communications in Mass Spectrometry* 19:1381–1391. doi:10.1002/rcm.1912.
- Bellasio C, Farquhar GD. 2019. A leaf-level biochemical model simulating the introduction of C₂ and C₄ photosynthesis in C₃ rice: gains, losses and metabolite fluxes. *New Phytologist* 223:150–166. doi:10.1111/nph.15787.
- Berveiller D, Damesin C. 2008. Carbon assimilation by tree stems: potential involvement of phosphoenolpyruvate carboxylase. *Trees* 22:149–157. doi:10.1007/s00468-007-0193-4.
- Berveiller D, Kierzkowski D, Damesin C. 2007. Interspecific variability of stem photosynthesis among tree species. *Tree Physiology* 27:53–61. doi:10.1093/treephys/27.1.53.
- Bianconi ME, Hackel J, Vorontsova MS, Alberti A, Arthan W, Burke SV, Duvall MR, Kellogg EA, Lavergne S, McKain MR, et al. 2020.

- Continued adaptation of C_4 photosynthesis after an initial burst of changes in the *Andropogoneae* grasses. *Systematic Biology* 69:445–461. doi:10.1093/sysbio/syz066.
- Bowling DR, Pataki DE, Randerson JT. 2008. Carbon isotopes in terrestrial ecosystem pools and CO_2 fluxes. *New Phytologist* 178:24–40. doi:10.1111/j.1469-8137.2007.02342.x.
- Cernusak LA, Marshall JD. 2000. Photosynthetic refixation in branches of Western white pine. *Functional Ecology* 14:300–311. doi:10.1046/j.1365-2435.2000.00436.x.
- Cernusak LA, Tcherkez G, Keitel C, Cornwell WK, Santiago LS, Knohl A, Barbour MM, Williams DG, Reich PB, Ellsworth DS, et al. 2009. Viewpoint: why are non-photosynthetic tissues generally ^{13}C enriched compared with leaves in C_3 plants? Review and synthesis of current hypotheses. *Functional Plant Biology* 36:199–213. doi:10.1071/FP08216.
- Chang WJ, Chang MJ, Chang ST, Yeh TF. 2013. Chemical composition and immunohistological variations of a growing bamboo shoot. *Journal of Wood Chemistry and Technology* 33:144–155. doi:10.1080/02773813.2013.769114.
- Chen M, Guo L, Ramakrishnan M, Fei Z, Vinod KK, Ding Y, Jiao C, Gao Z, Zha R, Wang C, et al. 2022. Rapid growth of Moso bamboo (*Phyllostachys edulis*): cellular roadmaps, transcriptome dynamics, and environmental factors. *Plant Cell* 34:3577–3610. doi:10.1093/plcell/koac193.
- Chen M, Ju Y, Ahmad Z, Yin Z, Ding Y, Que F, Yan J, Chu J, Wei Q. 2021. Multi-analysis of sheath senescence provides new insights into bamboo shoot development at the fast growth stage. *Tree Physiology* 41:491–507. doi:10.1093/treephys/tpaa140.
- Coplen TB, Brand WA, Gehre M, Gröning M, Meijer HAJ, Toman B, Verkouteren RM. 2006. New guidelines for $\delta^{13}C$ measurements. *Analytical Chemistry* 78:2439–2441. doi:10.1021/ac052027c.
- Damesin C. 2003. Respiration and photosynthesis characteristics of current-year stems of *Fagus sylvatica*: from the seasonal pattern to an annual balance. *New Phytologist* 158:465–475.
- Damesin C, Lelarge C. 2003. Carbon isotope composition of current-year shoots from *Fagus sylvatica* in relation to growth, respiration and use of reserves. *Plant, Cell & Environment* 26:207–219. doi:10.1046/j.1365-3040.2003.00951.x.
- Deleens E, Garnier-Dardart J. 1977. Carbon isotope composition of biochemical fractions isolated from leaves of *Bryophyllum daigremontianum bergeri*, a plant with crassulacean acid metabolism: some physiological aspects related to CO_2 dark fixation. *Planta* 135:241–248. doi:10.1007/BF00384896.
- Desalme D, Priault P, Gérard D, Dannoura M, Maillard P, Plain C, Epron D. 2017. Seasonal variations drive short-term dynamics and partitioning of recently assimilated carbon in the foliage of adult beech and pine. *New Phytologist* 213:140–153. doi:10.1111/nph.14124.
- Gessler A, Keitel C, Kodama N, Weston C, Winters AJ, Keith H, Grice K, Leuning R, Farquhar GD. 2007. $\delta^{13}C$ of organic matter transported from the leaves to the roots in *Eucalyptus delegatensis*: short-term variations and relation to respired CO_2 . *Functional Plant Biology* 34:692–706. doi:10.1071/FP07064.
- Gessler A, Ferrio JP, Hommel R, Treydte K, Werner RA, Monson RK. 2014. Stable isotopes in tree rings: towards a mechanistic understanding of isotope fractionation and mixing processes from the leaves to the wood. *Tree Physiology* 34:796–818. doi:10.1093/treephys/tpu040.
- Gessler A, Tcherkez G, Karyanto O, Keitel C, Ferrio JP, Ghashghaie J, Kreuzwieser J, Farquhar GD. 2009. On the metabolic origin of the carbon isotope composition of CO_2 evolved from darkened light-acclimated leaves in *Ricinus communis*. *New Phytologist* 181:374–386. doi:10.1111/j.1469-8137.2008.02672.x.
- Gessler A, Tcherkez G, Peuke AD, Ghashghaie J, Farquhar GD. 2008. Experimental evidence for diel variations of the carbon isotope composition in leaf, stem and phloem sap organic matter in *Ricinus communis*. *Plant, Cell and Environment* 31:941–953.
- Ghashghaie J, Badeck FW. 2014. Opposite carbon isotope discrimination during dark respiration in leaves versus roots—a review. *New Phytologist* 201:751–769. doi:10.1111/nph.12563.
- Ghashghaie J, Badeck FW, Lanigan G, Nogués S, Tcherkez G, Deleens E, Cornic G, Griffiths H. 2003. Carbon isotope fractionation during dark respiration and photorespiration in C_3 plants. *Phytochemistry Reviews* 2:145–161.
- Gilbert A, Robins RJ, Remaud GS, Tcherkez GGB. 2012. Intramolecular ^{13}C pattern in hexoses from autotrophic and heterotrophic C_3 plant tissues. *Proceedings of the National Academy of Sciences of the United States of America* 109:18204–18209. doi:10.1073/pnas.1211149109.
- Hanba YT, Kobayashi T, Enomoto T. 2010. Variations in the foliar $\delta^{13}C$ and C_3/C_4 species richness in the Japanese flora of Poaceae among climates and habitat types under human activity. *Ecological Research* 25:213–224. doi:10.1007/s11284-009-0652-z.
- Helle G, Schleser G. 2004. Beyond CO_2 fixation by Rubisco—an interpretation of $^{13}C/^{12}C$ variations in tree rings from novel intra-seasonal studies on broad-leaf trees. *Plant, Cell & Environment* 27:367–380. doi:10.1111/j.0016-8025.2003.01159.x.
- Hibberd JM, Quick WP. 2002. Characteristics of C_4 photosynthesis in stems and petioles of C_3 flowering plants. *Nature* 415:451–454. doi:10.1038/415451a.
- Höll W. 1974. Dark CO_2 fixation by cell-free preparations of the wood of *Robinia pseudoacacia*. *Canadian Journal of Botany* 52:727–734. doi:10.1139/b74-094.
- Kiyama S. 1905. About the gas inside the bamboo culms. *Tokyo Kagaku Kaishi* 26:333–357. doi:10.1246/nikkashi1880.26.333.
- Kodama N, Barnard RL, Salmon Y, Weston C, Ferrio JP, Holst J, Werner RA, Saurer M, Rennenberg H, Buchmann N, et al. 2008. Temporal dynamics of the carbon isotope composition in a *Pinus sylvestris* stand: from newly assimilated organic carbon to respired carbon dioxide. *Oecologia* 156:737–750. doi:10.1007/s00442-008-1030-1.
- Langenfeld-Heyser R. 1989. CO_2 fixation in stem slices of *Picea abies* (L.) Karst: microautoradiographic studies. *Trees* 3:24–32. doi:10.1007/BF00202397.
- Li X, Ye C, Fang D, Zeng Q, Cai Y, Du H, Mei T, Zhou G. 2022. Non-structural carbohydrate and water dynamics of Moso bamboo during its explosive growth period. *Frontiers in Forests and Global Change* 5:938941. doi:10.3389/fgc.2022.9389.
- Lundgren MR, Christin PA, Escobar EG, Ripley BS, Besnard G, Long CM, Hattersley PW, Ellis RP, Leegood RC, Osborne CP. 2016. Evolutionary implications of C_3 – C_4 intermediates in the grass *Alloteropsis semialata*. *Plant, Cell & Environment* 39:1874–1885. doi:10.1111/pce.12665.
- Müller R, Baier M, Kaiser WM. 1991. Differential stimulation of PEP-carboxylation in guard cells and mesophyll cells by ammonium and fusicoccin. *Journal of Experimental Botany* 42:215–220. doi:10.1093/jxb/42.2.215.
- Nalborczyk E. 1978. Dark carboxylation and its possible effect on the values of $\delta^{13}C$ in C_3 plants. *Acta Physiologiae Plantarum* 1:53–58.
- Porra RJ, Thompson WA, Kriedemann PE. 1989. Determination of accurate extinction coefficients and simultaneous equations for assaying chlorophylls *a* and *b* extracted with four different solvents: verification of the concentration of chlorophyll standards by atomic absorption spectroscopy. *Biochimica et Biophysica Acta - Bioenergetics* 975:384–394. doi:10.1016/S0005-2728(89)80347-0.
- Qi H, Coplen TB, Geilmann H, Brand WA, Böhlke JK. 2003. Two new organic reference materials for $\delta^{13}C$ and $\delta^{15}N$ measurements and a new value for the $\delta^{13}C$ of NBS 22 oil. *Rapid Communications in Mass Spectrometry* 17:2483–2487. doi:10.1002/rcm.1219.
- Qi H, Coplen TB, Mroczkowski SJ, Brand WA, Brandes L, Geilmann H, Schimmelmann A. 2016. A new organic reference material, L-glutamic acid, USGS41a for $\delta^{13}C$ and $\delta^{15}N$ measurements—a replacement for USGS41. *Rapid Communications in Mass Spectrometry* 30:859–866. doi:10.1002/rcm.7510.
- R Core Team. 2023. *R: a language and environment for statistical computing, v.4.2.2*. Vienna, Austria: R foundation for Statistical Computing. <http://www.r-project.org>
- Reed AH, Henry RJ, Mason WB. 1971. Influence of statistical method used on the resulting estimate of normal range. *Clinical Chemistry* 17:275–284. doi:10.1093/clinchem/17.4.275.

- Richter A, Wanek W, Werner RA, Ghashghaie J, Jäggi M, Gessler A, Brugnoli E, Hettmann E, Göttlicher SG, Salmon Y, et al. 2009. Preparation of starch and soluble sugars of plant material for the analysis of carbon isotope composition: a comparison of methods. *Rapid Communications in Mass Spectrometry* 23:2476–2488. doi:10.1002/rcm.4088.
- Rossmann A, Butzenlechner M, Schmidt HL. 1991. Evidence for a nonstatistical carbon isotope distribution in natural glucose. *Plant Physiology* 96:609–614. doi:10.1104/pp.96.2.609.
- Shi J, Mao S, Wang L, Ye X, Wu J, Wang G, Chen F, Yang Q. 2021. Clonal integration driven by source-sink relationships is constrained by rhizome branching architecture in a running bamboo species (*Phyllostachys glauca*): a ¹⁵N assessment in the field. *Forest Ecology and Management* 481:118754. doi:10.1016/j.foreco.2020.118754.
- Shi M, Zhang J, Sun J, Li Q, Lin X, Song X. 2022. Unequal nitrogen translocation pattern caused by clonal integration between connected ramets ensures necessary nitrogen supply for young Moso bamboo growth. *Environmental and Experimental Botany* 200:104900. doi:10.1016/j.envexpbot.2022.104900.
- Smith RG, Gauthier DA, Dennis DT, Turpin DH. 1992. Malate- and pyruvate-dependent fatty acid synthesis in leucoplasts from developing castor endosperm. *Plant Physiology* 98:1233–1238. doi:10.1104/pp.98.4.1233.
- Song X, Peng C, Zhou G, Gu H, Li Q, Zhang C. 2016. Dynamic allocation and transfer of non-structural carbohydrates, a possible mechanism for the explosive growth of Moso bamboo (*Phyllostachys heterocycla*). *Scientific Reports* 6:25908. doi:10.1038/srep25908.
- Tcherkez G, Nogués S, Bleton J, Cornic G, Badeck F, Ghashghaie J. 2003. Metabolic origin of carbon isotope composition of leaf dark-respired CO₂ in French Bean. *Plant Physiology* 131:237–244. doi:10.1104/pp.013078.
- Uchida EM, Katayama A, Yasuda Y, Enoki T, Otsuki K, Koga S, Utsumi Y. 2022. Age-related changes in culm respiration of *Phyllostachys pubescens* culms with their anatomical and morphological traits. *Frontiers in Forests and Global Change* 5:868732. doi:10.3389/ffgc.2022.868732.
- Vuorinen AH, Kaiser WM. 1997. Dark CO₂ fixation by roots of wild and barley in media with a high level of inorganic carbon. *Journal of Plant Physiology* 151:405–408. doi:10.1016/S0176-1617(97)80004-1.
- Wanek W, Heintel S, Richter A. 2001. Preparation of starch and other carbon fractions from higher plant leaves for stable carbon isotope analysis. *Rapid Communications in Mass Spectrometry* 15:1136–1140. doi:10.1002/rcm.353.
- Wang L, Li Q, Gao P, Wei S, Lu J, Gao Y, Zhang R. 2021. Activities of key enzymes involved in photosynthesis and expression patterns of corresponding genes during rapid growth of *Phyllostachys edulis*. *Journal of Zhejiang A&F University* 38:84–92. doi:10.11833/j.issn.2095-0756.20200277.
- Wang S, Chen TH, Liu EU, Liu CP. 2020. Accessing the nursing behaviour of Moso bamboo (*Phyllostachys edulis*) on carbohydrates dynamics and photosystems. *Scientific Reports* 10:1015. doi:10.1038/s41598-020-57643-1.
- Wang X, Liu L, Zhang J, Wang Y, Wen G, Gao R, Gao Y, Zhang R. 2012. Changes of photosynthetic pigment and photosynthetic enzyme activity in stems of *Phyllostachys pubescens* during rapid growth stage after shooting. *Chinese Journal of Plant Ecology* 36:456–462. doi:10.3724/SP.J.1258.2012.00456.
- Wittmann C, Hans M, van Winden WA, Ras C, Heijnen JJ. 2005. Dynamics of intracellular metabolites of glycolysis and TCA cycle during cell-cycle-related oscillation in *Saccharomyces cerevisiae*. *Biotechnology and Bioengineering* 89:839–847. doi:10.1002/bit.20408.
- Yen TM. 2016. Culm height development, biomass accumulation and carbon storage in an initial growth stage for a fast growing Moso bamboo (*Phyllostachys pubescens*). *Botanical Studies* 57:10. doi:10.1186/s40529-016-0126-x.
- Yen TM, Lee JS. 2011. Comparing aboveground carbon sequestration between Moso bamboo (*Phyllostachys heterocycla*) and China fir (*Cunninghamia lanceolata*) forests based on the allometric model. *Forest Ecology and Management* 261:995–1002. doi:10.1016/j.foreco.2010.12.015.
- Zachariah EJ, Sabulal B, Nair DNK, Johnson AJ, Kumar CSP. 2016. Carbon dioxide emission from bamboo culms. *Plant Biology* 18:400–405. doi:10.1111/plb.12435.
- Zhai W, Wang Y, Luan J, Liu S. 2022. Effects of nitrogen addition on clonal integration between mother and daughter ramets of Moso bamboo: a ¹³C-CO₂ pulse labeling study Zhang W-H (ed). *Journal of Plant Ecology* 15:756–770. doi:10.1093/jpe/rtab115.
- Zhang M, Chen S, Jiang H, Cao Q. 2020. The water transport profile of *Phyllostachys edulis* during the explosive growth phase of bamboo shoots. *Global Ecology and Conservation* 24:e01251. doi:10.1016/j.gecco.2020.e01251.